CHEMISTRY OF MATERIALS
Article

Chem. Mater. **2010,** *22,* 5695–5699 5695
DOI:10.1021/cm102187a

Decoration, Migration, and Aggregation of Palladium Nanoparticles on Graphene Sheets

Zhong Jin,[†] David Nackashi,[‡] Wei Lu,[†] Carter Kittrell,[†] and James M. Tour*[,†]

[†]*Departments of Chemistry and Mechanical Engineering and Materials Science, The Smalley Institute for Nanoscale Science and Technology, Rice University, MS-222, 6100 Main Street, Houston, Texas 77005, and* [‡]*Protochips Inc., 617 Hutton Street, Suite 111, Raleigh, North Carolina 27606*

Received August 2, 2010. Revised Manuscript Received September 8, 2010

As a two-dimensional carbon nanomaterial, graphene has a high surface area and good chemical stability; therefore, its potential applicability in composite materials and as a catalyst support is high. Here, we report a facile process to decorate graphene sheets with well-dispersed Pd nanoparticles. By the in situ formation and adhesion of Pd nanoparticles to the thermally exfoliated graphene (TEG) sheets suspended in a solvent, a Pd/TEG composite was prepared and characterized by transmission electron microscopy, X-ray photoelectron spectroscopy, and Brunauer−Emmett−Teller (BET) surface area analysis. The migration and aggregation of Pd nanoparticles on the graphene sheets was directly observed by scanning transmission electron microscopy. As the composite was heated to 700 °C, there was little movement of the Pd nanoparticles; on heating to 800 °C, well below the melting temperature, the Pd nanoparticles began to migrate, coalesce, and agglomerate to form larger particles. The aggregation behavior was further confirmed by X-ray diffraction analysis of the Pd/TEG composite before and after being annealed at 800 °C. The graphene sheets provided a real-time imaging platform with nanometer-scale thickness to study the thermal stability and migratory behavior of nanoscale materials.

Introduction

Graphene, as a two-dimensional nanomaterial of sp^2-hybridized carbon, has attracted increasing interest due to its great potential for applications in electronic devices and composite materials.[1,2] Moreover, with high surface area and good chemical stability, graphene can be used as gas absorbant,[3] ultracapacitor material,[4] or support material for developing novel heterogeneous catalysts with enhanced activity.[5] Recently, there have been some reports on the use of graphene or graphite oxide-based materials serving as supports for noble metal nanoparticles, such as Ag,[6−8] Pd,[9−15] Pt,[5,16−23] and Au.[24,25] Among these noble metals, Pd nanoparticles are especially important for their extensive catalytic applications in organic reactions[26−29] such as hydrogenation,[9,10,30,31] hydrosilylation,[32] Suzuki−Miyaura coupling reaction,[13,15,33,34] Heck

*To whom correspondence should be addressed. E-mail: tour@rice.edu.

(1) Novoselov, K. S.; Geim, A. K.; Morozov, S. V.; Jiang, D.; Zhang, Y.; Dubonos, S. V.; Grigorieva, I. V.; Firsov, A. A. *Science* **2004**, *306*, 666.
(2) Stankovich, S.; Dikin, D. A.; Dommett, G. H. B.; Kohlhaas, K. M.; Zimney, E. J.; Stach, E. A.; Piner, R. D.; Nguyen, S. T.; Ruoff, R. S. *Nature* **2006**, *442*, 282.
(3) Ghosh, A.; Subrahmanyam, K. S.; Krishna, K. S.; Datta, S.; Govindaraj, A.; Pati, S. K.; Rao, C. N. R. *J. Phys. Chem. C* **2008**, *112*, 15704.
(4) Stoller, M. D.; Park, S. J.; Zhu, Y. W.; An, J. H.; Ruoff, R. S. *Nano Lett.* **2008**, *8*, 3498.
(5) Yoo, E.; Okata, T.; Akita, T.; Kohyama, M.; Nakamura, J.; Honma, I. *Nano Lett.* **2009**, *9*, 2255.
(6) Lu, G. H.; Mao, S.; Park, S.; Ruoff, R. S.; Chen, J. H. *Nano Research* **2009**, *2*, 192.
(7) Zhou, X. Z.; Huang, X.; Qi, X. Y.; Wu, S. X.; Xue, C.; Boey, F. Y. C.; Yan, Q. Y.; Chen, P.; Zhang, H. *J. Phys. Chem. C* **2009**, *113*, 10842.
(8) Lightcap, I. V.; Kosel, T. H.; Kamat, P. V. *Nano Lett.* **2010**, *10*, 577.
(9) Mastalir, A.; Kiraly, Z.; Benko, M.; Dekany, I. *Catal. Lett.* **2008**, *124*, 34.
(10) Mastalir, A.; Kiraly, Z.; Patzko, A.; Dekany, I.; L'Argentiere, P. *Carbon* **2008**, *46*, 1631.
(11) Gotoh, K.; Kawabata, K.; Fujii, E.; Morishige, K.; Kinumoto, T.; Miyazaki, Y.; Ishida, H. *Carbon* **2009**, *47*, 2120.
(12) Hassan, H. M. A.; Abdelsayed, V.; Khder, A.; AbouZeid, K. M.; Terner, J.; El-Shall, M. S.; Al-Resayes, S. I.; El-Azhary, A. A. *J. Mater. Chem.* **2009**, *19*, 3832.
(13) Scheuermann, G. M.; Rumi, L.; Steurer, P.; Bannwarth, W.; Mulhaupt, R. *J. Am. Chem. Soc.* **2009**, *131*, 8262.
(14) Hu, Z. L.; Aizawa, M.; Wang, Z. M.; Yoshizawa, N.; Hatori, H. *Langmuir* **2010**, *26*, 6681.
(15) Li, Y.; Fan, X.; Qi, J.; Ji, J.; Wang, S.; Zhang, G.; Zhang, F. *Nano Res.* **2010**, *3*, 429−437.
(16) Si, Y. C.; Samulski, E. T. *Chem. Mater.* **2008**, *20*, 6792.
(17) Kou, R.; Shao, Y. Y.; Wang, D. H.; Engelhard, M. H.; Kwak, J. H.; Wang, J.; Viswanathan, V. V.; Wang, C. M.; Lin, Y. H.; Wang, Y.; Aksay, I. A.; Liu, J. *Electrochem. Commun.* **2009**, *11*, 954.
(18) Li, Y. M.; Tang, L. H.; Li, J. H. *Electrochem. Commun.* **2009**, *11*, 846.
(19) Seger, B.; Kamat, P. V. *J. Phys. Chem. C* **2009**, *113*, 7990.
(20) Dong, L. F.; Gari, R. R. S.; Li, Z.; Craig, M. M.; Hou, S. F. *Carbon* **2010**, *48*, 781.
(21) Li, Y. J.; Gao, W.; Ci, L. J.; Wang, C. M.; Ajayan, P. M. *Carbon* **2010**, *48*, 1124.
(22) Liu, S.; Wang, J. Q.; Zeng, J.; Ou, J. F.; Li, Z. P.; Liu, X. H.; Yang, S. R. *J. Power Sources* **2010**, *195*, 4628.
(23) Shao, Y. Y.; Zhang, S.; Wang, C. M.; Nie, Z. M.; Liu, J.; Wang, Y.; Lin, Y. H. *J. Power Sources* **2010**, *195*, 4600.
(24) Muszynski, R.; Seger, B.; Kamat, P. V. *J. Phys. Chem. C* **2008**, *112*, 5263.
(25) Kamat, P. V. *J. Phys. Chem. Lett.* **2010**, *1*, 520.
(28) Choudary, B. M.; Madhi, S.; Chowdari, N. S.; Kantam, M. L.; Sreedhar, B. *J. Am. Chem. Soc.* **2002**, *124*, 14127.
(29) Zhang, Z. H.; Wang, Z. Y. *J. Org. Chem.* **2006**, *71*, 7485.
(30) Studer, M.; Blaser, H. U.; Exner, C. *Adv. Synth. Catal.* **2003**, *345*, 45.

Published on Web 09/24/2010

coupling reaction,[35,36] Stille coupling reaction,[37,38] and Wacker oxidation.[39] However, the morphology and dispersion of Pd nanoparticles may be changed by heating;[40] surface restructuring, interdiffusion, and sintering of Pd nanoparticles can also be observed after annealing at relatively low temperature (~425 °C) on normal support materials such as silica or alumina, which will decrease the performance of gas adsorption and catalytic applications.[40−42] Therefore, it is essential to investigate the thermal stability and robustness of Pd nanoparticles on support materials at high temperature. A key factor of the stability of metal nanoparticles is the rate of aggregation and coalescence; graphene sheets can provide an excellent platform for the direct imaging of the migration behavior of nanoparticles. Here, we report a facile process to decorate well-dispersed Pd nanoparticles on thermally exfoliated graphene (TEG) sheets. This Pd/TEG composite was obtained by the in situ reduction of palladium(II) acetate by hydrazine hydrate in a suspension of TEG sheets under mild conditions; no protective agent or surfactant was used. Thus, the Pd/TEG composite could be prepared with minimal contamination. The morphology and dispersion of Pd nanoparticles on graphene sheets was investigated. The migration and aggregation behavior of Pd nanoparticles at high temperature was monitored in real time by scanning transmission electron microscopy (STEM).

Experimental Section

Preparation of the Pd/TEG Composite. The TEG material was obtained by rapid thermal-expansion of graphite oxide (GO, synthesized by Hummers method[43]) at 1000 °C under a H_2/Ar (50 sccm/500 sccm) gas flow.[44,45] Then, the TEG was annealed at 1000 °C for 15 min in the H_2/Ar gas flow. In this modified procedure, most of the oxygen content in TEG was removed by the H_2 treatment. The process of the decoration of palladium nanoparticles on TEG sheets is shown in Scheme 1. Typically, TEG (24 mg, 2 meqiv carbon) and tetrahydrofuran (THF, 40 mL) were placed in a 100 mL round-bottom flask and tip-sonicated for 30 min with a Misonix 3000 probe sonicator at 30 W. Then, palladium(II) acetate (4.0 mg, 0.018 mmol) was dissolved in the TEG suspension. Under vigorous stirring, hydrazine hydrate (5 μL, 0.10 mmol) was added into the suspension, and the mixture was stirred for 1 h. After the reaction, one drop of 30% hydrogen peroxide was added to remove the excess hydrazine hydrate. The mixture was filtered over a polycarbonate membrane (0.22 μm pore size), and the filter cake was rinsed twice with 50 mL of THF. After washing, the Pd/TEG composite was dried at 80 °C in a vacuum oven at 30 mmHg.

Scheme 1. Decoration of Palladium Nanoparticles on TEG Sheets and Coalescence of Pd at 800 °C

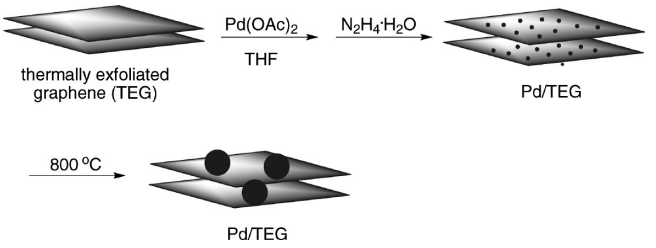

Characterizations. The Pd/TEG composite was characterized by transmission electron microscopy (TEM), X-ray photoelectron spectroscopy (XPS), Brunauer−Emmett−Teller (BET) surface area analysis, scanning transmission electron microscopy (STEM), and X-ray diffraction (XRD). For TEM and STEM measurements, the Pd/TEG composite powder was directly applied to blank copper microgrids without any lacy carbon film. TEM characterizations and selected-area electron diffraction (SAED) patterns were completed on a JEOL 2100F field emission gun transmission electron microscope. XPS analysis was carried out on a PHI Quantera SXM Scanning X-ray Microprobe with a pass energy of 140.00 eV (survey scan) or 26.00 eV (high resolution scan), 45° takeoff angle, and 100 μm beam size. Multipoint BET measurements were taken using 11 points on a Quantachrome Autosorb-3b BET surface analyzer with liquid nitrogen at 77 K. For the real-time observation of the migration of Pd nanoparticles at different temperatures, STEM was carried out with a Hitachi SU-6600 FESEM, which was equipped with an Aduro ultrafast heating stage for high temperature analysis. The Aduro heating stage is capable of reaching temperatures from ambient to 1200 °C and has accurate temperature control of the samples. XRD data were collected with a Rigaku D/Max Ultima II using Cu Ka radiation (k = 0.15406 nm) at 40 kV and 40 mA.

Results and Discussion

The as-obtained Pd nanoparticles were well-dispersed on the surface of the graphene sheets, as shown in the high-resolution TEM (HRTEM) images (Figure 1). The size distribution of the Pd nanoparticles, as determined by HRTEM, was ~2.0−5.6 nm. The mean size of the Pd nanoparticles decorated on the graphene sheets was ~4.1 nm. The HRTEM image (Figure 1b) shows the spacing of the lattice fringes (0.225 nm) of two Pd nanoparticles, which corresponds to the Pd (111) crystalline planes.

The weight percentage of Pd nanoparticles in the Pd/TEG composite was measured by XPS analysis, as shown in Figure 2. The two peaks centered at 335.5 and 341.0 eV can be assigned to $Pd3d_{5/2}$ and $Pd3d_{3/2}$, respectively,[13,15,46]

(31) Zhao, M. Q.; Crooks, R. M. *Angew. Chem., Int. Ed.* **1999**, *38*, 364.
(32) Horn, K. A. *Chem. Rev.* **1995**, *95*, 1317.
(33) Suzuki, A. *J. Organomet. Chem.* **1999**, *576*, 147.
(34) Narayanan, R.; El-Sayed, M. A. *J. Am. Chem. Soc.* **2003**, *125*, 8340.
(35) Reetz, M. T.; Breinbauer, R.; Wanninger, K. *Tetrahedron Lett.* **1996**, *37*, 4499.
(36) Cassol, C. C.; Umpierre, A. P.; Machado, G.; Wolke, S. I.; Dupont, J. *J. Am. Chem. Soc.* **2005**, *127*, 3298.
(37) Stille, J. K. *Angew. Chem., Int. Ed.* **1986**, *25*, 508.
(38) Roth, G. P.; Farina, V.; Liebeskind, L. S.; Penacabrera, E. *Tetrahedron Lett.* **1995**, *36*, 2191.
(39) Mitsudome, T.; Umetani, T.; Mori, K.; Mizugaki, T.; Ebitani, K.; Kaneda, K. *Tetrahedron Lett.* **2006**, *47*, 1425.
(40) Lu, J. L.; Weissenrieder, J.; Kaya, S.; Gao, H. J.; Shaikhutdinov, S.; Freund, H. J. *Surf. Rev. Lett.* **2007**, *14*, 927.
(41) Heemeier, M.; Stempel, S.; Shaikhutdinov, S. K.; Libuda, J.; Baumer, M.; Oldman, R. J.; Jackson, S. D.; Freund, H. J. *Surf. Sci.* **2003**, *523*, 103.
(42) Min, B. K.; Santra, A. K.; Goodman, D. W. *J. Vac. Sci. Technol., B* **2003**, *21*, 2319.
(43) Hummers, W. S.; Offeman, R. E. *J. Am. Chem. Soc.* **1958**, *80*, 1339.
(44) Schniepp, H. C.; Li, J. L.; McAllister, M. J.; Sai, H.; Herrera-Alonso, M.; Adamson, D. H.; Prud'homme, R. K.; Car, R.; Saville, D. A.; Aksay, I. A. *J. Phys. Chem. B* **2006**, *110*, 8535.
(45) McAllister, M. J.; Li, J. L.; Adamson, D. H.; Schniepp, H. C.; Abdala, A. A.; Liu, J.; Herrera-Alonso, M.; Milius, D. L.; CarO, R.; Prud'homme, R. K.; Aksay, I. A. *Chem. Mater.* **2007**, *19*, 4396.
(46) Moulder, J. F.; Stickle, W. F.; Sobol, P. E.; Bomben, K. D. *Handbook of X-ray Photoelectron Spectroscopy*; Chastain, J., Ed.; Physical Electronics Division, Perkin-Elmer Corporation: Eden Prairie, MN, 1992.

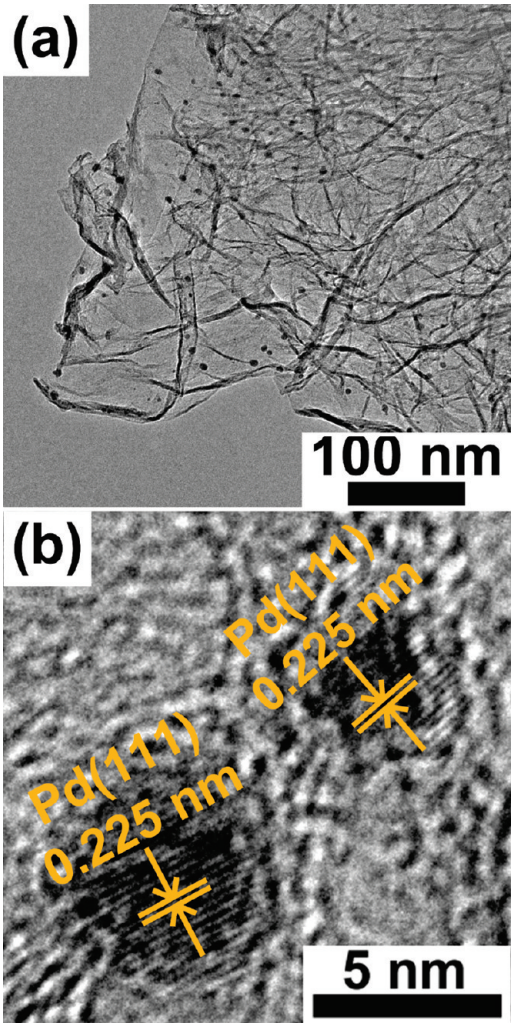

Figure 1. (a) TEM and (b) high-resolution TEM images of Pd nanoparticles decorated on graphene sheets. (b) The spacing of lattice fringes in the two Pd nanoparticles is 0.225 nm, which can be attributed to the Pd(111) crystalline planes.

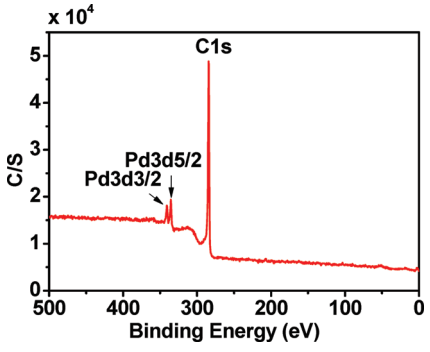

Figure 2. XPS spectrum of the Pd/TEG composite. The binding energies of $Pd3d_{5/2}$ and $Pd3d_{3/2}$ peaks are at 335.5 and 341.0 eV, respectively.

which indicates the presence of Pd metal in the product. High-resolution XPS scan of the Pd/TEG composite shows the atomic percentage of Pd was ~0.9%, which is ~7.5 wt %. The XPS atomic percentage of Pd in the Pd/TEG is comparable with the mole percentage of palladium(II) acetate in the reagents, indicating that almost all of the palladium(II) acetate had been reduced to Pd nanoparticles and captured by the surface of the graphene sheets.

The specific surface area of the original TEG material and Pd/TEG composite were measured by BET nitrogen adsorption after degassing at 120 °C for 16 h. The surface area of original TEG material was found to be as high as 550 $m^2 \cdot g^{-1}$. The Pd/TEG composite had surface areas of ~450 $m^2 \cdot g^{-1}$, which indicates that the surface area of TEG has been well preserved. It is possible that the Pd nanoparticles kept the spacing between the graphene sheets by functioning as "spacers"; thus, the specific surface area in the 2-D graphene structure was retained.[16]

The migration of Pd nanoparticles at high temperature was directly observed by STEM. The temperature of the Pd/TEG composite sample was accurately controlled by an Aduro heating stage. Until the temperature reached 700 °C, the Pd nanoparticles did not appear to move and were without any obvious aggregation. On heating to 800 °C, the Pd particles began to migrate on the graphene sheets, as shown in Figure 3. A STEM movie of the migration and aggregation of Pd nanoparticles is online at YouTube.[47] About 10 min after the temperature reached 800 °C, the Pd nanoparticles began to move closer to each other. Once in contact, the Pd nanoparticles coalesced in order to reduce their surface energy.[48] The contacted Pd nanoparticles first formed a short thin bridge between each other, followed by slow growth of the width of the bridge; then finally, the smaller particles merged to a larger particle with a spherical shape. It was also observed that smaller nanoparticles were absorbed by the larger ones, a typical Ostwald ripening phenomenon.[49] Migration distances exceeding 100 nm were observed. In this way, the individual nanosized Pd nanoparticles gradually merged and agglomerated to particles with larger size. In 30 min, the Pd nanoparticles in the visual range of STEM observation had congregated to form several large particles with diameters up to ~20 nm. Moreover, to investigate the intermediate stages of the coalescence process of Pd nanoparticles, the Pd/TEG composite was annealed at 800 °C in H_2/Ar (200 sccm/200 sccm) gas flow for 18 min. As shown in the Supporting Information S1, the "bridged" Pd nanoparticles at different intermediate states of the aggregation can be observed by TEM after annealing, which provides additional evidence to support the coalescence mechanism and to depict how two or more Pd nanoparticles formed the "necks" at the aggregation sites outlined in Figure 3.

XRD analysis was used to further investigate the change in size of the Pd nanoparticles at high temperature, as shown in Figure 4. The XRD pattern of the as-obtained Pd/TEG composite is shown in Figure 4a, and the diffraction peak ~25.9° is attributed to the (002) reflection of a few-layered graphene structure. Several peaks were observed in the XRD pattern at 40.4°, ~46.8°, ~68.3°, and ~82.2°. These peaks correspond to the (111), (200), (220), and (311) planes of a face-centered cubic (fcc)

(47) A STEM movie of the migration and aggregation of Pd nanoparticles on graphene sheets can be found on YouTube, http://www.youtube.com/watch?v=iEcbHSGHATw.
(48) Lim, T. H.; McCarthy, D.; Hendy, S. C.; Stevens, K. J.; Brown, S. A.; Tilley, R. D. *ACS Nano* **2009**, *3*, 3809.
(49) Palasantzas, G.; Vystavel, T.; Koch, S. A.; De Hosson, J. T. M. *J. Appl. Phys.* **2006**, 99.

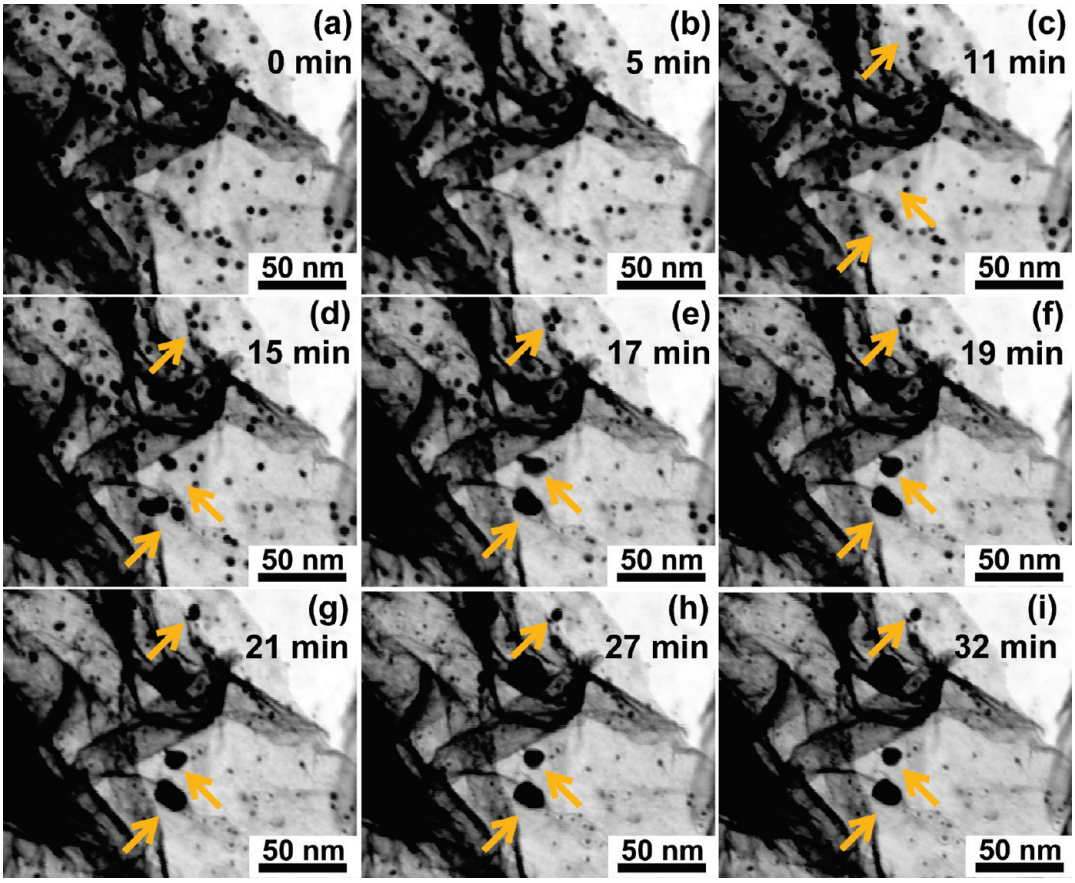

Figure 3. (a−i) STEM images of the Pd nanoparticles on graphene sheets; the self-migration of Pd nanoparticles at 800 °C was monitored in real time and recorded at the designated time values for each frame. The aggregation sites of some of the Pd nanoparticles are shown by yellow arrows.

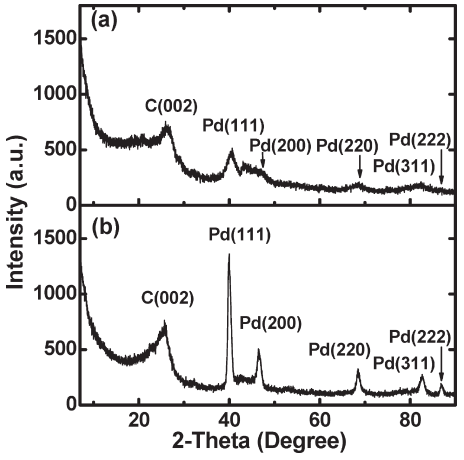

Figure 4. XRD spectra of the (a) as-obtained Pd/TEG composite and (b) after annealing at 800 °C in Ar/H_2 gas flow for 30 min.

lattice, respectively, indicating that the Pd nanoparticles synthesized in this study have the fcc crystal structure. For a comparative experiment, the Pd/TEG composite was annealed at 800 °C in H_2/Ar (200 sccm/200 sccm) gas flow for 30 min. As shown in Figure 4b, the annealed Pd/TEG composite had an XRD pattern with significantly sharper peaks than the XRD pattern of the as-obtained Pd/TEG composite without annealing, and the peak at ~86.8°, corresponding to the Pd(222) planes, was also observed, indicating that larger Pd nanoparticles were present on the graphene sheets. The mean sizes of Pd nanoparticles on the as-obtained and annealed Pd/TEG composites were calculated to be ~4.0 and 13.9 nm, respectively, from the broadening of the Pd(220) diffraction peaks using the Scherrer's equation.[50] The increased size of the Pd nanoparticles characterized by the XRD analysis is comparable to the size change observed by STEM, which supports the conclusion that the aggregation of Pd nanoparticles occurred not only in the field of view of the STEM[47] but also in the bulk material. Furthermore, the selected-area electron diffraction (SAED) patterns of Pd/TEG composite before and after annealing at 800 °C were, respectively, collected with TEM, as shown in Supporting Information S2. The intensity change of Pd(222) diffraction rings in the SAED patterns is consistent with the intensity change of Pd(222) peaks in the XRD spectra (Figure 4), which gives supplementary evidence that the average size of Pd nanoparticles in the composite has been increased by annealing.

Summary

In conclusion, we developed a facile process to decorate graphene sheets with well-dispersed Pd nanoparticles by the in situ preparation and adhesion of Pd nanoparticles to the suspension of TEG. The morphology and components of Pd/TEG composite were characterized by TEM,

(50) Cullity, B. D.; Stock, S. R. *Elements of X-Ray Diffraction*, 3rd Ed.; Prentice-Hall Inc.: Upper Saddle River, NJ, 2001; p 167.

XPS, and BET nitrogen adsorption. The migration of Pd nanoparticles at high temperature was directly observed by STEM, which showed that the Pd nanoparticles were stable at 700 °C but coalesced and agglomerated to particles with larger size at 800 °C.[47] The excellent thermal stability of Pd/graphene composite is beneficial for the further heterogeneous catalytic application. It was also indicated that graphene sheets could be used as a two-dimensional platform with nanometer-scale thickness for the direct real-time observation of the thermal stability and migratory behavior of nanoscale materials.

Acknowledgment. Financial support was provided by the U.S. Department of Energy's Office of Energy Efficiency and Renewable Energy within the Hydrogen Sorption Center of Excellence at the National Renewable Energy Laboratory, DEFC-36-05GO15073.

Supporting Information Available: The HRTEM images of Pd nanoparticles on TEG sheets after annealing at 800 °C for 18 min in Ar/H_2 gas flow, the SAED patterns of Pd/TEG composite before and after annealing at 800 °C for 30 min in Ar/H_2 gas flow (PDF). This material is available free of charge via the Internet at http://pubs.acs.org.